Bioorg. Med. Chem. 28 (2020) 115810

Contents lists available at ScienceDirect

Bioorganic & Medicinal Chemistry

journal homepage: www.elsevier.com/locate/bmc

Preventing *Candida albicans* biofilm formation using aromatic-rich piperazines

Gaëlle Simon [a,b,1], Christopher Bérubé [a,1], Pierre-Alexandre Paquet-Côté [a], Daniel Grenier [b], Normand Voyer [a,*]

[a] Département de Chimie and PROTEO, Université Laval, 1045 Avenue de la Médecine, Québec, QC G1V 0A6, Canada
[b] Groupe de Recherche en Écologie Buccale, Faculté de Médecine Dentaire, Université Laval, 2420 Rue de la Terrasse, Québec, QC G1V 0A6, Canada

ARTICLE INFO

Keywords:
Piperazines
Candida albicans
Antibiofilm
Morphological switching
Oxime resin

ABSTRACT

The global increase in microbial resistance is an imminent threat to public health. Effective treatment of infectious diseases now requires new antimicrobial therapies. We report herein the discovery of aromatic-rich piperazines that inhibit biofilm formation by *C. albicans*. 22 piperazines, including 16 novel ones, were prepared efficiently using a combination of solid- and solution phase synthesis. The most potent compound prevents morphological switching under several hypha-inducing conditions and reduces *C. albicans'* ability to adhere to epithelial cells. These processes are essential to the development of *Candida* biofilms, which are associated with its increased resistance to immune defenses and antifungal agents.

1. Introduction

Candida albicans, a commensal microorganism that colonizes the human mucosa, is an opportunistic pathogen that can cause various infections[1] ranging from superficial dermal or mucosal infections, such as candidiasis[2,3] and denture stomatitis,[4] to often-deadly bloodstream infections.[5] This fungus represents a serious threat, especially for immunocompromised individuals[6] and for healthy patients with implanted medical devices,[7,8] including heart valves and pacemakers, prostheses, dentures and catheters.[9] In fact, *C. albicans* is the main fungus responsible for medical-device-associated infections, and *Candida* species are the third-most frequent causal agents of sepsis, accounting for 15% of all nosocomial bloodstream infections.[1,10] Colonization of medical devices, mucosa, and tooth enamel by *C. albicans* is closely associated with its ability to adhere to, and form biofilms on, these surfaces.

Indeed, it forms highly structured biofilms that harbor multiple cell types, including budded round cells (yeast) and elongated joint cells such as hyphae and intermediate pseudohyphae.[11] It has been shown that *C. albicans* can switch from one morphotype to another in response to specific environmental conditions, a process called morphogenesis.[12] Each morphology is implicated in a different step of biofilm development, which all play critical roles in *C. albicans* virulence and pathogenesis.[13]

On the other hand, the biofilm life cycle is initiated by the adherence of yeast to a surface, followed by proliferation until a basal layer is formed. Then, the biofilm matures through the elongation of hyphae and secretion of extracellular matrix components.[1] Finally, the yeast is released, which disperses the biofilm to colonize new areas.[14]

Considering the socioeconomic burden of *Candida* medical-device-associated infections[15–18] and the resistance of fungal biofilms to drugs,[19–22] the development of novel therapies based on new modes of action is imperative.[6,23-25] Small molecules that interfere with morphogenesis could be useful adjuvants for antifungal therapies.

The piperazine ring is the fourth most frequent heterocyclic scaffold found in drugs.[26] Piperazines are well known for their wide range of bioactivities[27] and can be synthesized by reduction of 1,4-diketopiperazines, a class of cyclic dipeptides (CDPs) often reported for anti-biofilm properties.[28,29] Herein, we report the synthesis of a series of 22 piperazines, including 16 novel ones (Figure 1) and their anti-biofilm formation against *C. albicans*.

* Corresponding author.
E-mail address: normand.voyer@chm.ulaval.ca (N. Voyer).
[1] These authors contributed equally.

https://doi.org/10.1016/j.bmc.2020.115810
Received 19 July 2020; Received in revised form 4 October 2020; Accepted 5 October 2020
Available online 9 October 2020
0968-0896/© 2020 Elsevier Ltd. All rights reserved.

2. Results

2.1. Synthesis of piperazine analogs

Based on the possibility of synthesizing rapidly aromatic CDPs,[30] a series of piperazines was prepared using L- or D-phenylalanine and tyrosine following the general procedure illustrated in Figure 1. A noteworthy feature of our synthetic approach is the efficient solid-phase preparation of chiral CDPs from readily available *N*-Boc protected amino acids,[31–34] which can be converted to the corresponding piperazines.

A set of 22 piperazines (**1**–**5**) and *N,N'*-dimethyl-piperazines (**1′-5′**) with various stereochemistries and aromatic substituents was synthesized to allow structure–activity investigations. Briefly, the synthesis started by coupling the first amino acid on the oxime resin[35,36] for three hours using diisopropylcarbodiimide (DIC) as coupling reagent. The *N*-Boc protecting group was removed using a mixture of 1:1 trifluoroacetic acid (TFA)/dichloromethane. The second amino acid was coupled using 6-chlorohydroxybenzotriazole (6-Cl-HOBt) and (2-(6-Chloro-1H-benzotriazole-1-yl)-1,1,3,3-tetramethylaminium hexafluorophosphate (HCTU). After deprotection, the linear dipeptide was simultaneously cyclized and cleaved from the resin in the presence of diisopropylethylamine (DIEA; 2.5 equiv) and acetic acid (AcOH; 5 equiv) in dichloromethane, leading to high-purity CDPs. Using this synthetic procedure, we successfully synthesized CDPs with a variety of chiral cis and trans side chains. A total of 9 CDPs were prepared and characterized by ^{1}H NMR, ^{13}C NMR and mass spectrometry analyses.[31,32] Then, piperazine analogs were readily produced by the reduction of the CDPs using an excess of lithium aluminum hydride in THF at reflux for 24–72 h. The key to a successful reduction here is the treatment of the crude reduction mixture with sodium sulfate decahydrate for 30 min (Figure 1).[37,38] Aromatic piperazines **1**, **3**, **5** were obtained with 80% to 87% yields. Following the reduction step, a part of the cis piperazines bearing protected phenol side chains (**1a, 1b, 3a and 3b**) were immediately subjected to hydrogenolysis using H_2 and Pd on charcoal as

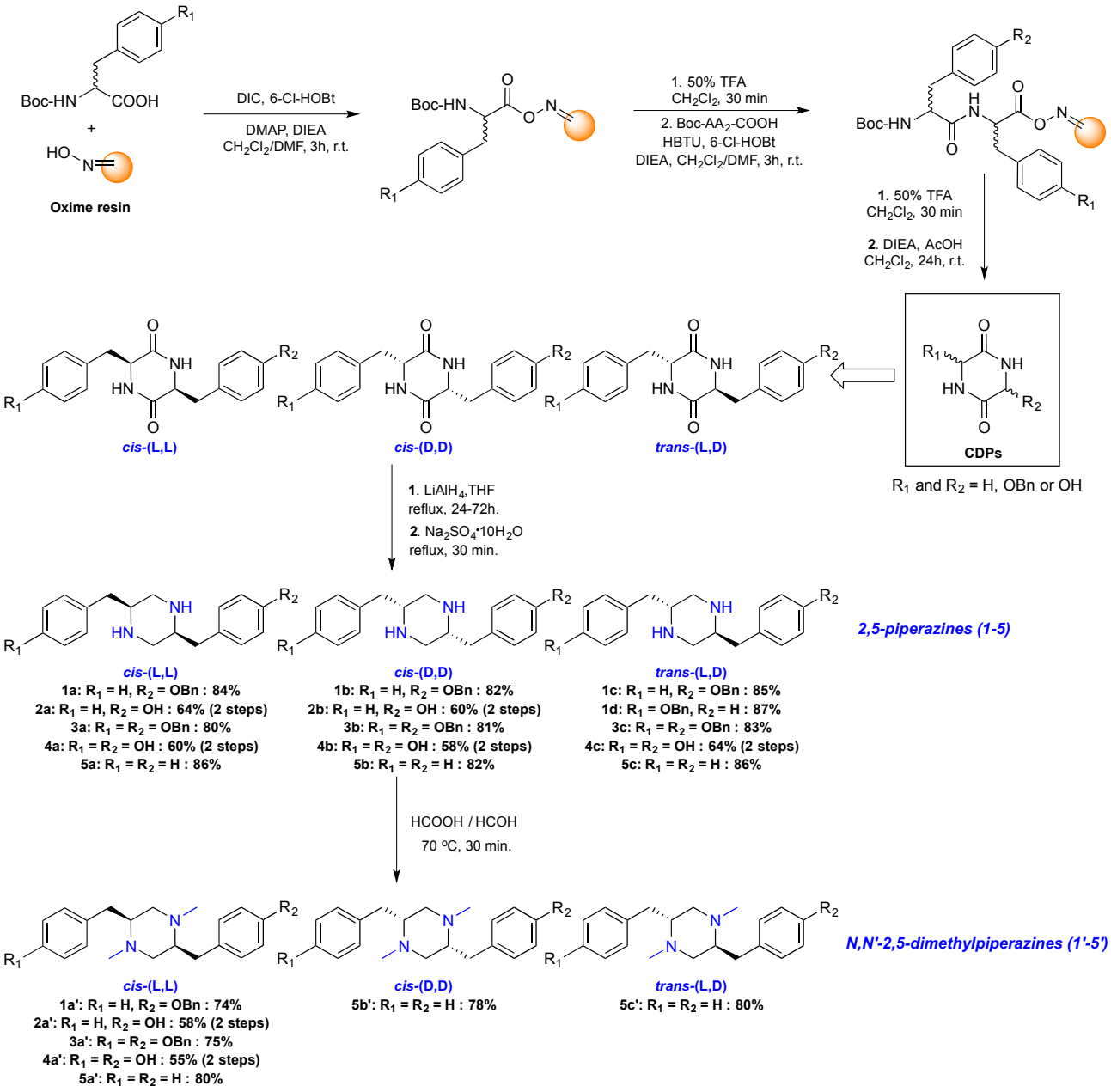

Figure 1. Synthesis of piperazines (1–5), and their *N,N*-dimethylated analogs (1′-5′) under investigations.

catalyst, leading to compounds **2** and **4** with 58% to 64% yields for the two steps. *N*-methylation of piperazines using the Eschweiler–Clarke reaction led to the *N,N'*-dimethyl-piperazines **1'**, **3'** and **5'** with 74% to 80% yields.[39] To obtain *N,N'*-dimethylated compounds with unprotected phenol **2a'** and **4a'**, the OBn-protected precursors **1a** and **3a** were subjected to double *N*-methylation followed by a final hydrogenolysis. Their respective overall yields are 58% and 55% after the double *N*-methylation and hydrogenolysis steps respectively. Characterization of the 2,5-piperazines and their *N,N'*-dimethylated analogs is available in the Supplementary data (Figure S1–S41).

2.2. Antibiofilm activity

The antibiofilm activity was evaluated against *C. albicans* ATCC 28,366 at piperazine concentrations up to 96 μg/mL. The piperazines made only from phenylalanine residues (**5a-c, 5a'-c'**) were inactive and therefore will not be discussed. Overall, compounds **1a-1c** and **3a-3c** were the most effective inhibitors of *C. albicans* biofilm formation.

Piperazine **1a** significantly inhibited biofilm formation ($p < 0.01$) at a concentration as low as 1 μg/mL (Figure 2A). Additional experiments were performed using the clinical isolate LAM-1, a wild strain from a sepsis patient. There was significant inhibition of *C. albicans* LAM-1 biofilm formation in the presence of 4 μg/mL of **1a** (Figure 2B). Altogether, the antibiofilm activity of piperazine **1a** against *C. albicans* was observed at concentrations 25- to 100-fold lower than the minimal inhibitory concentration (MIC = 96 μg/mL) that was obtained under the same experimental conditions. Piperazines **1a-d** did not impede yeast growth and viability at concentrations up to 64 μg/mL, as shown by the measurement of optical density at 660 nm (OD_{660}) and by the plate count determination.

Although similar concentration ranges of all four stereoisomers of piperazine **1** inhibited fungal biofilm formation (Figure 3), compound **1d** exhibited the weakest antibiofilm and antifungal activities (MIC > 128 μg/mL). Piperazine **1d** is also less soluble than compounds **1a-c**, which may contribute to the lower activity observed. The *N*-methylated analog **1a'** was inactive (data not shown). This indicates that the N—H groups are involved in the antibiofilm mechanism of action. In addition, free hydroxyl analogs (**2a-b**) had no effect on fungal growth and biofilm

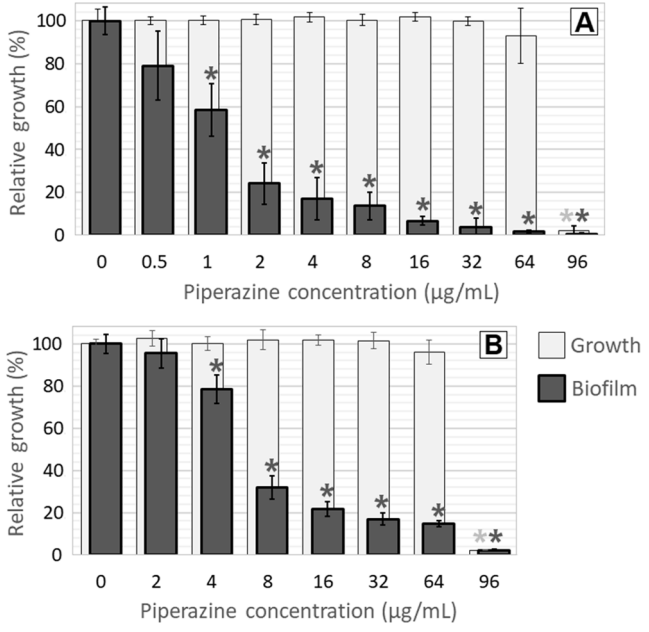

Figure 2. Fungal growth and biofilm formation by *C. albicans* ATCC 28,366 (A) and LAM-1 (B) in the presence of piperazine **1a**. Data are represented as mean ± standard deviation. (* $p < 0.01$).

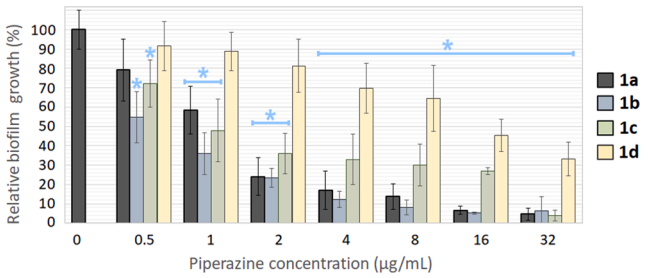

Figure 3. Biofilm formation by *C. albicans* ATCC 28,366 in the presence of **1a-1d**. Data are represented as mean ± standard deviation. (* $p < 0.01$).

formation (data not shown). Therefore, the large hydrophobic benzyl groups are required for bioactivity.

Compared to piperazines **1**, compounds with two benzyl ether moieties (**3**) showed a slightly lower antibiofilm properties (Figure 4a). Inhibition of biofilm formation was significantly measured at 2 μg/mL for compounds **3a-3b** (Figure 4A), making their antibiofilm activity effective at concentrations about 12-fold less than the MIC-. Indeed, compounds with a *cis* configuration **3a-b** have better antifungal activities, with MIC and minimum fungicidal concentrations (MFC) of 24 μg/mL under the experimental biofilm conditions.

The *trans* isomer **3c** was less potent than its analogs and did not impede fungal growth at the concentration range tested (MIC > 128 μg/mL), but impeded biofilm formation at concentration of 48 μg/mL (Figure 4B). Removal of the benzyl group (**4a**, **4b**) and/or *N*-methylation (**3a'**, **4a'**) of these compounds suppressed all activity, therefore confirming the proposed involvement of the N—H groups and importance of the benzyl ether for activity.

Surprisingly, *N*-methylated compound **2a'** with only one free hydroxyl led to a weak antibiofilm activity at concentrations of 24 to 96 μg/mL (Figure 4C). Considering the distant structural analogy that relates compound **2a'** with the other antibiofilm piperazines, its activity is thought to use a different mechanism. As the MIC of **2a'** was significantly higher than those of the other compounds, no specific investigation was conducted to shed light on its possible mode of action.

Although eight compounds that prevent *C. albicans* biofilm development were identified, no piperazine was effective in disrupting a preformed biofilm (data not shown). These findings suggest that the molecules interfere with the normal life cycle of the biofilm, but do not have the ability to affect the mature biofilm and its polymeric matrix.

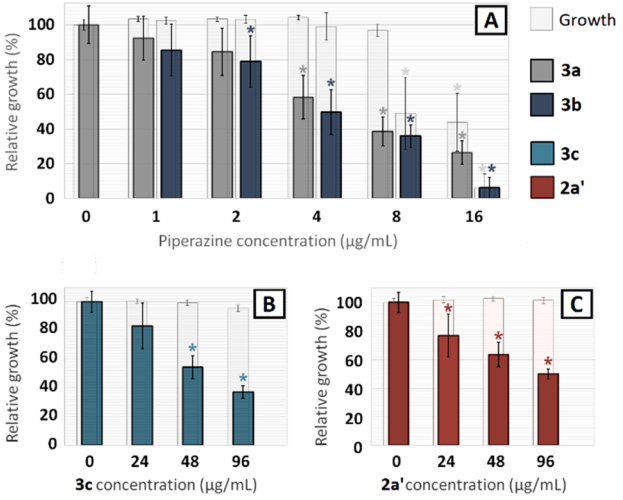

Figure 4. Fungal growth and biofilm formation by *C. albicans* ATCC 28,366 in the presence of (A) cis piperazines **3a** and **3b**; (B) trans piperazine **3c**;(C) *N,N'*-dimethyl-piperazine **2a'**. Data are represented as mean ± standard deviation. (* $p < 0.01$).

2.3. Antibiofilm mechanisms of action of piperazines

To investigate the mechanism of action of the antibiofilm activity of piperazine **1a** on *C. albicans*, we studied its impact on morphogenesis and cell adherence, two on the main processes involved in the life cycle of the fungus and in the biofilm formation.[40,41]

2.4. Inhibition of C. Albicans morphogenesis

C. albicans remains in the budded morphotype when grown at 30 °C in Yeast Extract-Peptone-Dextrose broth (YPD). Its morphogenesis can be initiated by using appropriate hyphae-inducing culture media.[12,42–44]

The impact of piperazine **1a** on *C. albicans*' ability to form hyphae was studied by microscopy after 4 h of growth in Spider medium (Figure 5), a carbon deprivation environment which stimulates formation of hyphae. No real hyphae cells were present after incubation with 4 μg/mL of piperazine **1a** (Figure 5 D). The first real hyphae cells to be observed were short and represented only a small subpopulation of the culture grown with 2 μg/mL of piperazine **1a** (Figure 5C). Even though filamentation effectively led to the elongation of joint hypha cells in the presence of 1 μg/mL of **1a** in Spider medium (Figure 5B), their appearance was still remarkably distinct from the positive control (Figure 5A) and an important proportion of pseudohyphae and intermediate morphologies were present.

The cells were counted as hypha or yeast to determine the percentage of individuals that underwent morphological changes. This count confirmed that the morphogenesis of *C. albicans* ATCC 28,366 was significantly inhibited in Spider medium ($p < 0.01$) in the presence of compounds **1a** and **1b** at the lowest antibiofilm concentrations (Figure 6). A comparable activity level was observed using the clinical strain LAM-1. With both strains there was no activity using twice as much of the *N*- methylated piperazine **1a'**, suggesting that the N—H groups also play a key role in morphogenesis inhibition. The measure of OD_{660} and a further plate count after incubation confirmed that the growth and viability of *C. albicans* were not affected by the piperazines in this experiment. This indicates that the inhibition of filamentation by these compounds does not result from their fungicidal activity.

The ability of compound **1a** to inhibit morphogenesis was investigated further in other hyphae-inducing media (Figure 7).[42,43] Inhibition of filamentation was significantly observed starting from 2 μg/mL in

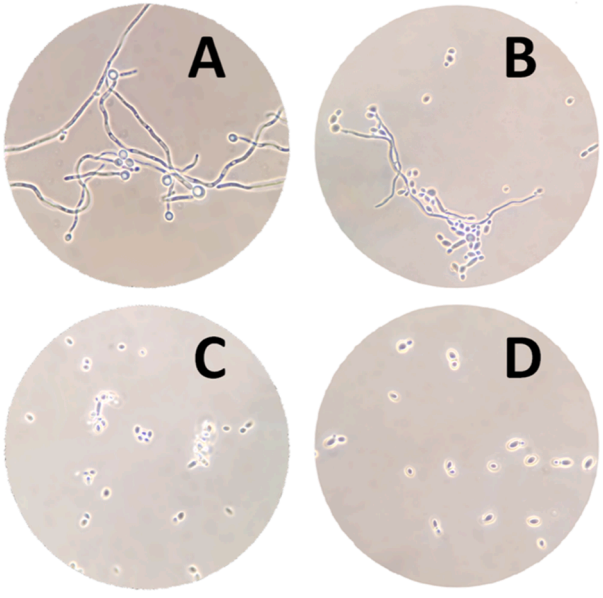

Figure 5. Morphology of *C. albicans* ATCC 28,366 after incubation in Spider medium with piperazine **1a** at concentrations of (A) 0 μg/mL;(B) 1 μg/mL; (C) 2 μg/mL; (D) 4 μg/mL.

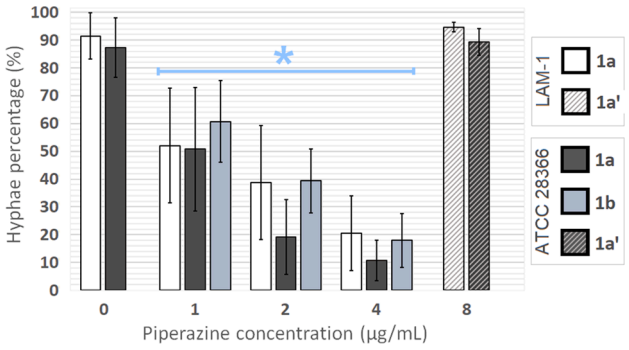

Figure 6. Proportion of *C. albicans* LAM-1 (white) and ATCC 28,366 (color) cells in the hypha morphology after 4 h of incubation in Spider medium in the presence of piperazine **1** analogs. Data are represented as mean ± standard deviation. (* $p < 0.01$).

Lee's medium, an amino acid deprived medium.[45] In addition, piperazine **1a** at 1 μg/mL inhibited morphological switching in YPD despite supplementation with 10% fetal bovine serum (FBS), which strongly induces morphogenesis. Finally, piperazine **1a** had no effect on morphological switching induced by *N*-acetylglucosamine as the only carbon source (GlcNAc 0.5%) or by nitrogen deprivation (SLAD). Methylation of the amine functions of **1a** (**1a'**) resulted in the loss of activity for Lee's media and YDP + 10% FBS or no activity for the GlcNAc 0.5% and SLAD conditions.

These results were obtained within 4 h of incubation of a diluted culture and demonstrate an inhibition of filamentation in the early exponential growth phase. Experiments do not prove that filamentation impairment occurs under the biofilm conditions or under dense population. It should be noted that the rise in temperature from 30 to 37 °C alone can initiate the filamentation of yeast cultured in YPD. This experimental factor was reproduced in each experiment above and its potential contribution cannot be quantified. The characterization of grown biofilms by scanning electron microscopy would provide evidence of this effect under biofilm-forming conditions and would help determine whether the inhibition of morphogenesis contributes to antibiofilm activity.

2.5. Adherence to epithelial cells

Adherence to a surface is the initial step of biofilm development and a key process for pathogenesis and tissue infection. Consequently, genes and regulators involved in adhesion often contribute to biofilm formation among other vital elements, such as cell wall integrity.[46] To determine if the antibiofilm piperazine **1a** could also inhibit the first step of biofilm establishment, adherence of *C. albicans* ATCC 28,366 on oral epithelial cells GMSM-K was evaluated by fluorescence microscopy using microorganisms labeled with fluorescein-isothiocyanate (FITC) after 4 h of incubation (Figure 8). Clearly, the adherence of *C. albicans* decreases significantly in the presence of piperazine **1a**. A dose-dependent reduction of fungal adherence to epithelial cells was observed in the antibiofilm concentration range, starting from 6 μg/mL of **1a** ($p < 0.01$) (Figure 9).

2.6. In vitro biocompatibility with oral epithelial cells

In view of a potential therapeutic use of piperazine **1a**, its biocompatibility was assessed using an oral epithelial cell model. Human oral epithelial cells (cell line B11) were treated with various concentrations of piperazine **1a** for 2 and 24 h prior to monitor cell viability using a MTT (3-[4, 5-diethylthiazol-2-yl]-2,5-diphenyltetrazolium bromide) assay. Results showed that following a 2-h treatment, only the highest concentration (96 μg/mL) of piperazine **1a** significantly decreases the cell viability. When the treatment was extended to 24 h, a significant

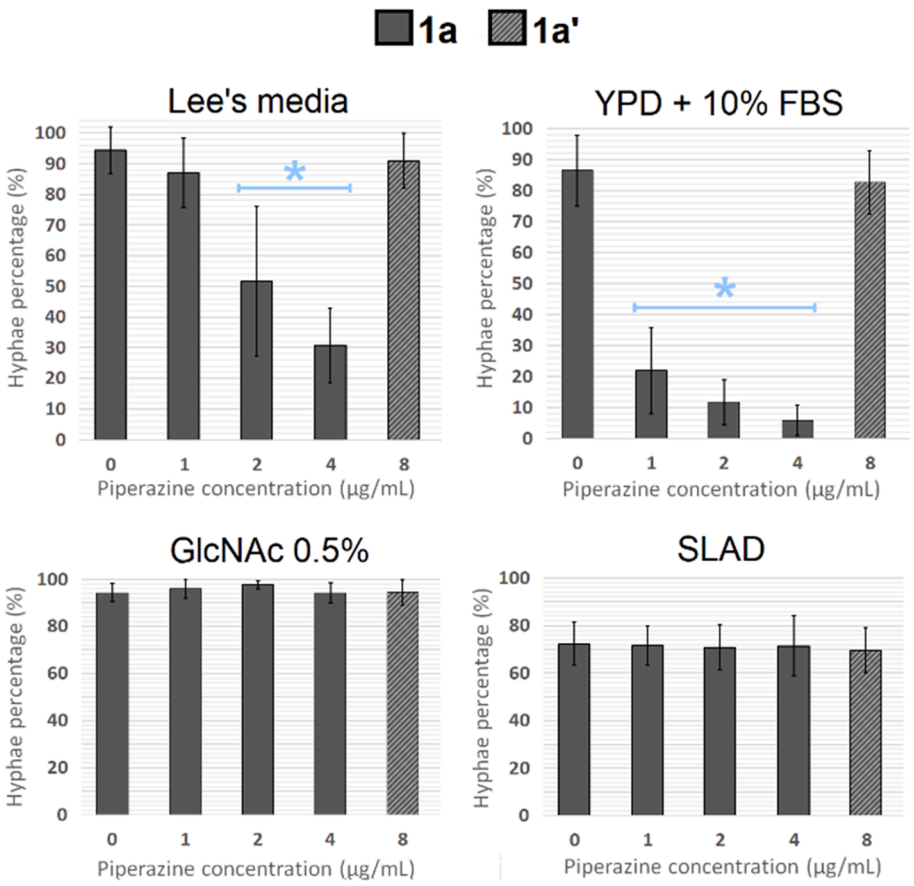

Figure 7. Morphological switching in *C. albicans* ATCC 28,366 yeast cells induced using different hypha-inducing culture media in the presence of piperazines **1a** and **1a'**. Data are represented as mean ± standard deviation. (* $p < 0.01$).

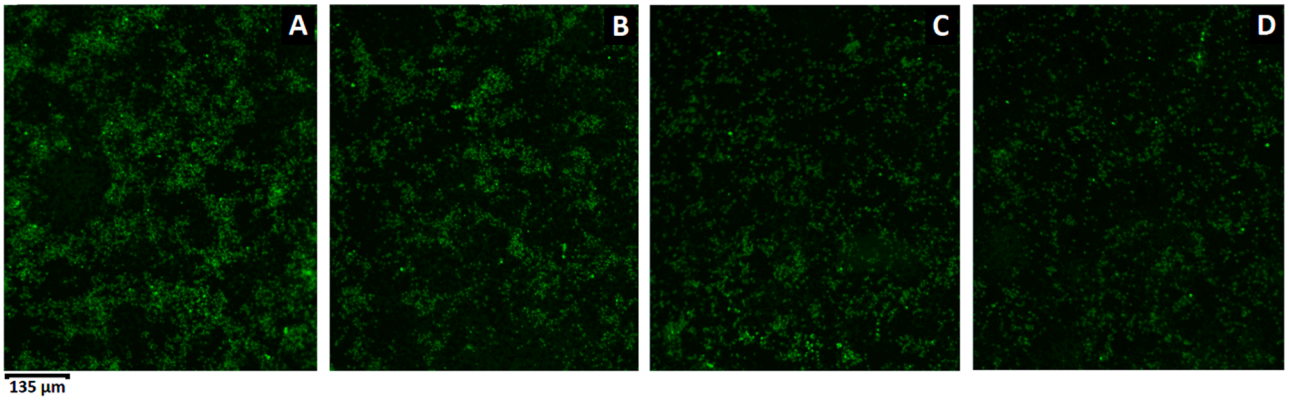

Figure 8. Adherence of FITC-labeled *C. albicans* to GMSM-K epithelial cells with piperazine **1a** at concentrations of (A) 0 µg/mL; (B) 12 µg/mL; (C) 24 µg/mL; (D) 48 µg/mL.

reduction in cell viability was observed at concentrations ≥ 24 µg/mL (Figure 10).

3. Discussion

Over 2000 genes[47] and 50 transcriptional regulators[48] are implicated in biofilm formation by *C. albicans* through the different stages of biofilm development, in which the cells adopt differentiated gene expression. A core transcriptional network of nine regulators was identified among the complex set of interconnected metabolic pathways required for biofilm development.[47,49,50] Most of them are also involved in the regulation of adherence, morphological switching,[40] extracellular matrix production, biofilm dispersion, degradation enzymes secretion, and other virulence factors.[41,51] These processes are influenced, and therefore can be controlled, by environmental cues and small molecules.[12–49,52] On this basis, we have studied the effect of piperazine **1a** on *C. albicans* morphological switching and adherence.

In this study, we have synthesized 22 piperazines, including 16 new piperazines and identified eight that inhibit biofilm formation by *C. albicans* without affecting planktonic growth. Structure-activity relationship studies reveal the importance of the benzyl ether moiety present in antibiofilm piperazines **1** and **3**. Analogs with free hydroxyls (**2**, **4**) were inactive. *N*-methylation of the antibiofilm compounds also resulted in a loss of activity, suggesting the participation of the N—H

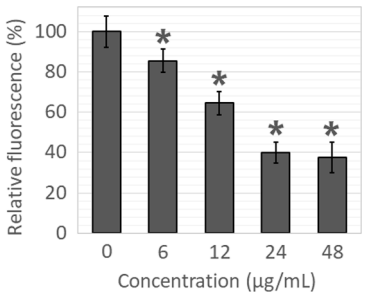

Figure 9. Relative fluorescence of FITC-labeled *C. albicans* adhered to GMSM-K epithelial cells in the presence of piperazine **1a**. Data are represented as mean ± standard deviation. (* $p < 0.01$).

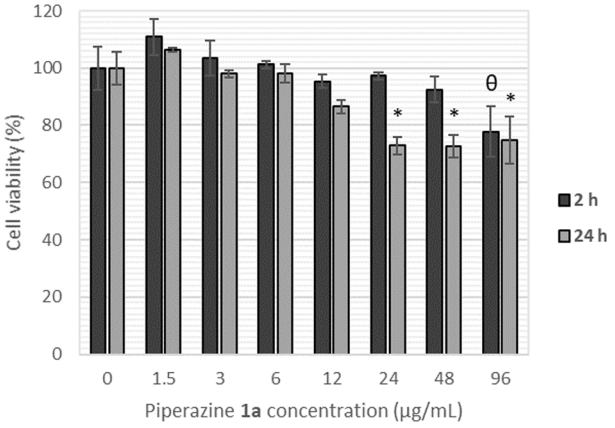

Figure 10. Cell viability of human oral epithelial cell line B11 in the presence of piperazine **1a** after 2 h and 24 h. Data are represented as mean ± standard deviation. (θ p between 0.01 and 0.001) (* $p < 0.001$).

groups in the mechanism of action. These results are in line with observations made during other antibiofilm activity studies of cyclic dipeptides, analogs of piperazines under investigation.[30] Notably, piperazines have better solubilities than their cyclic dipeptide analogs.

Microbial adherence is ensured by adhesion proteins and by non-specific physicochemical interactions as well. Environmental factors such as quorum-sensing molecules, colonization by other microorganisms, and even host hormones can influence the adhesion process,[53–56] which *in vitro* seems to mostly depend on the nature of the surface. The results reported show a significant reduction of adherence on epithelial cells by **1a**. However, it does not identify the reduction of adherence as a causal factor for the antibiofilm activity of compound **1a** at the conditions of the biofilm assay, as the biofilm adhered to a different material. The inhibition of fungal adherence to epithelial cells by **1a** demonstrates a supplementary and complementary mechanism of action by which the compound may inhibit biofilm development under biological conditions.

On the other hand, piperazine **1a** inhibits the morphological switching of *C. albicans* under two hyphae-inducing conditions. In Spider medium, the transcriptional regulator Efg1 induces hypha formation in response to carbon deprivation through Gpr1 in the cAMP-PKA pathway. Additionally, **1a** inhibits morphological switching in Lee's medium (Figure 7), in which the amino acid limitation activates the transcription factors Cph2 and Tec1 to upregulate filamentation genes.[43] Likewise, **1a** is also active in YPD with 10% of FBS (Figure 7). The FBS strongly induces morphogenesis through both MAPK and cAMP-PKA in response to activation of Ras GTPases.[57–59] However, piperazine **1a** had no effect on morphological switching induced by *N*-acetylglucosamine as the only carbon source (0.5% GlcNAc) or by nitrogen deprivation (SLAD), which respectively induce morphogenesis by activation of the transcription factor Cph1 via *N*-acetylglucosamine transporter Ngt1[60] or through the MAPK pathway,[51,61] although other regulators are involved.[50,62, 63,64] Thus, many targets might be suggested for the mechanisms through which piperazine **1a** inhibits *C. albicans* filamentation. Altogether, the results suggest that the piperazine interferes with the Ras-cAMP-PKA pathway and the upstream regulators of Tec1 and Efg1, core regulators of biofilm development.[40,49] Overall, inhibition of morphogenesis is likely to contribute to the antibiofilm activity of piperazines **1a-d**. Using mutant strains in the morphogenesis inhibition assay to systematically investigate the effect of gene depletion could lead to a better understanding of the precise sites where the piperazines interfere.

Compound **1a** was effective in reducing the ability of *C. albicans* to form a biofilm and to adhere to oral epithelial cells at relatively low concentrations. In addition, we showed that at concentrations required for anti-biofilm and anti-adhesion effects, compound **1a** did not affect the human cell viability following a 2-h exposure. These results are interesting in view of a potential therapeutic use of compound **1a** for treating/preventing *C. albicans* infections, even though toxicity at higher concentrations (≥24 µg/mL) after a 24-h exposure may limit its efficacy.

4. Conclusions

A set of 22 piperazines were synthesized efficiently and studied for their ability to inhibit biofilm formation by *C. albicans*. Some compounds alter biofilm-related processes far below their fungicidal concentration. Most importantly, piperazine **1a** inhibits the morphological switching of *C. albicans* and its adherence to epithelial cells at concentrations that does not reduce the cells viability.

Overall, considering the inhibition of the *C. albicans* biofilm-related processes and the highly interconnected mechanisms that regulate biofilm development, the piperazines may act as perturbators of metabolic or signaling pathways of the fungus. The action of **1a** is most probably through interferences with the Ras-cAMP-PKA pathway and the upstream regulators of Tec1 and Efg1, although more work is needed to pinpoint the exact mechanism of action.

It is believed that therapeutic strategies that do not result in the direct killing of pathogens would prevent the rise of resistance and reduce side effects of antimicrobial drugs.[65,66] Therefore, the results reported herein targeting metabolic pathways that regulate biofilm development and virulence expression with small aromatic-rich piperazines constitute an interesting avenue towards novel antifungal therapies.[67–70]

5. Experimental section

5.1. General information

Oxime resin, coupling reagents and *N*-Boc-protected amino acids were purchased from Matrix Innovation (Québec City, QC, Canada). Unless indicated otherwise, all chemicals were purchased from commercial sources and used directly. NMR spectra were recorded using Varian Inova 400 MHz and NMR Agilent DD2 500 MHz spectrometers. The coupling constants are reported in hertz (Hz). Chemical shifts are reported in parts per million (ppm) downfield from tetramethylsilane. Splitting patterns are designated as s (singlet), d (doublet), dd (doublet of doublets), t (triplet), q (quartet), br (broad) and m (multiplet). Mass spectra were obtained on an Agilent 6210 LC Time of Flight Mass Spectrometer in direct injection mode. Optical density and absorbance values for biofilm formation assays were obtained using a BIO-RAD xMark Microplate spectrophotometer. Adherence of *C. albicans* on epithelial cells was measured by fluorescence spectrometry using a Synergy 2 spectrophotometer (BioTek Instruments, USA) and pictures were taken with a FSX100 Olympus camera.

5.2. Synthesis

5.2.1. General procedures for the synthesis of 1,4-piperazines

All 1,4-piperazine (1-5a-c) were prepared from the corresponding cyclic dipeptides (CDPs). The latter were prepared by solid-phase peptide synthesis with oxime resin using the appropriate phenylalanine or tyrosine derivatives.[31,32] 1,4-Piperazines were readily produced by the reduction of CDPs using $LiAlH_4$ (1 M in THF) for 48 h in dry THF under an inert atmosphere. Once the reaction was completed, $Na_2SO_4{\cdot}10H_2O$ was added to neutralize residual $LiAlH_4$ and other active species, and the mixture was refluxed for 30 min.[37,38] Residual solids were eliminated by filtration which led to the desired crude aromatic 1,4-piperazines with 80% to 87% yields. Crude products were purified by flash chromatography using CH_2Cl_2/MeOH as eluent.

5.2.1.1. (2S,5S)-2-benzyl-5-(4-(benzyloxy)benzyl)piperazine (1a). Pale yellow powder, 84% yield. **mp** = 170 °C. **^{1}H NMR** (500 MHz, $CDCl_3$): δ 1.74 (s, 2H), 2.75 (dd, J = 13.4, 5.6 Hz, 1H), 2.81 (dd, J = 13.4, 5.6 Hz, 1H), 2.84–2.89 (m, 4H), 2.91–3.03 (m, 4H), 5.06 (s, 2H), 6.92–6.95 (m, 2H), 7.13–7.16 (m, 2H), 7.21–7.24 (m, 3H), 7.30–7.35 (m, 3H), 7.38–7.41 (m, 2H), 7.44–7.46 (m, 2H). **^{13}C NMR** (126 MHz, $CDCl_3$) δ 37.6, 38.5, 47.9, 48.0, 55.6, 55.7, 70.1, 114.9, 126.2, 127.5, 127.9, 128.5, 128.6, 129.2, 130.1, 131.2, 137.1, 139.3, 157.3. **HRMS** (ESI-TOF, m/z): calcd for $C_{25}H_{29}N_2O$ $(M + H)^+$ = 373.2274, found 373.2269. **HPLC** (retention time, purity): 23.45 min, 99%.

5.2.1.2. (2R,5R)-2-benzyl-5-(4-(benzyloxy)benzyl)piperazine (1b). White powder, 82% yield. **mp** = 170 °C. **^{1}H NMR** (500 MHz, $CDCl_3$): δ 1.74 (s, 2H), 2.75 (dd, J = 13.4, 5.6 Hz, 1H), 2.81 (dd, J = 13.4, 5.6 Hz, 1H), 2.84–2.89 (m, 4H), 2.91–3.03 (m, 4H), 5.06 (s, 2H), 6.92–6.95 (m, 2H), 7.13–7.16 (m, 2H), 7.21–7.24 (m, 3H), 7.30–7.35 (m, 3H), 7.38–7.41 (m, 2H), 7.44–7.46 (m, 2H). **^{13}C NMR** (126 MHz, $CDCl_3$) δ 37.6, 38.5, 47.9, 48.0, 55.6, 55.7, 70.1, 114.9, 126.2, 127.5, 127.9, 128.5, 128.6, 129.2, 130.1, 131.2, 137.1, 139.3, 157.3. **HRMS** (ESI-TOF, m/z): calcd for $C_{25}H_{29}N_2O$ $(M + H)^+$ = 373.2274, found 373.2259. **HPLC** (retention time, purity): 23.45 min, 99%.

5.2.1.3. (2S,5R)-2-benzyl-5-(4-(benzyloxy)benzyl)piperazine (1c). Pale yellow powder, 85% yield. **mp** = 171 °C. **^{1}H NMR** (500 MHz, $CDCl_3$): δ 2.43–2.48 (m, 3H), 2.53 (dd, J = 13.4, 8.6 Hz, 1H), 2.66 (ddd, J = 28.8, 13.5, 5.1 Hz, 2H), 2.82–2.92 (m, 2H), 2.96 (ddd, J = 11.4, 5.5, 2,7 Hz, 2H), 5.04 (s, 2H), 6.91 (d, J = 8.6 Hz, 2H), 7.10 (d, J = 8.6 Hz, 2H), 7.18–7.23 (m, 3H), 7.28–7.34 (m, 3H), 7.37–7.44 (m, 4H). **^{13}C NMR** (126 MHz, $CDCl_3$) δ 39.9, 40.8, 52.6, 52.7, 62.6, 70.0, 114.9, 126.4, 127.4, 127.9, 128.5, 129.2, 130.1, 137.0, 138.4, 157.4. **HRMS** (ESI-TOF, m/z): calcd for $C_{25}H_{29}N_2O$ $(M + H)^+$ = 373.2278, found 373.2269. **HPLC** (retention time, purity): 23.12 min, 97%.

5.2.1.4. (2R,5S)-2-benzyl-5-(4-(benzyloxy)benzyl)piperazine (1d). Pale yellow powder, 87% yield. **mp** = 171 °C. **^{1}H NMR** (500 MHz, $CDCl_3$): δ 2.43–2.48 (m, 3H), 2.53 (dd, J = 13.4, 8.6 Hz, 1H), 2.66 (ddd, J = 28.8, 13.5, 5.1 Hz, 2H), 2.82–2.92 (m, 2H), 2.96 (ddd, J = 11.4, 5.5, 2,7 Hz, 2H), 5.04 (s, 2H), 6.91 (d, J = 8.6 Hz, 2H), 7.10 (d, J = 8.6 Hz, 2H), 7.18–7.23 (m, 3H), 7.28–7.34 (m, 3H), 7.37–7.44 (m, 4H). **^{13}C NMR** (126 MHz, $CDCl_3$) δ 39.9, 40.8, 52.6, 52.7, 62.6, 70.0, 114.9, 126.4, 127.4, 127.9, 128.5, 129.2, 130.1, 137.0, 138.4, 157.4. **HRMS** (ESI-TOF, m/z): calcd for $C_{25}H_{29}N_2O$ $(M + H)^+$ = 373.2272, found 373.2269. **HPLC** (retention time, purity): 23.12 min, 97%.

5.2.1.5. (2S,5S)-2,5-bis(4-(benzyloxy)benzyl)piperazine (3a). White powder, 80% yield. **mp** = 135 °C. **^{1}H NMR** (400 MHz, DMSO-d_6): δ 1.80 (s, 2H), 2.50–2.57 (m, 4H), 2.58–2.63 (m, 6H), 5.01 (s, 4H), 6.87 (d, J = 8.3 Hz, 4H), 7.06 (d, J = 8.3 Hz, 4H), 7.27 (t, J = 7.1 Hz, 2H), 7.34 (t, J = 7.4 Hz, 4H), 7.39 (d, J = 7.4 Hz, 4H). **^{13}C NMR** (125 MHz, DMSO-d_6): δ 47.6, 55.9, 61.2, 69.6, 115.0, 128.1, 128.2, 128.9, 130.5, 132.6, 137.8, 157.0. **HRMS** (ESI-TOF, m/z) calcd for $C_{32}H_{35}N_2O_2$ $(M + H)^+$ = 479.2693, found 479.2688. **HPLC** (retention time, purity): 30.69 min, 99%.

5.2.1.6. (2R,5R)-2,5-bis(4-(benzyloxy)benzyl)piperazine (3b). White powder, 81% yield. **mp** = 135 °C. **^{1}H NMR** (400 MHz, DMSO-d_6): δ 1.80 (s, 2H), 2.50–2.57 (m, 4H), 2.58–2.63 (m, 6H), 5.01 (s, 4H), 6.87 (d, J = 8.3 Hz, 4H), 7.06 (d, J = 8.3 Hz, 4H), 7.27 (t, J = 7.1 Hz, 2H), 7.34 (t, J = 7.4 Hz, 4H), 7.39 (d, J = 7.4 Hz, 4H). **^{13}C NMR** (125 MHz, DMSO-d_6): δ 47.6, 55.9, 61.2, 69.6, 115.0, 128.1, 128.2, 128.9, 130.5, 132.6, 137.8, 157.0. **HRMS** (ESI-TOF, m/z) calcd for $C_{32}H_{35}N_2O_2$ $(M + H)^+$ = 479.2693, found 479.2700. **HPLC** (retention time, purity): 30.69 min, 95%.

5.2.1.7. (2S,5R)-2,5-bis(4-(benzyloxy)benzyl)piperazine (3c). White powder, 83% yield. **mp** = 135 °C. **^{1}H NMR** (400 MHz, DMSO-d_6): δ 1.80 (s, 2H), 2.50–2.57 (m, 4H), 2.58–2.63 (m, 6H), 5.01 (s, 4H), 6.87 (d, J = 8.3 Hz, 4H), 7.06 (d, J = 8.3 Hz, 4H), 7.27 (t, J = 7.1 Hz, 2H), 7.34 (t, J = 7.4 Hz, 4H), 7.39 (d, J = 7.4 Hz, 4H). **^{13}C NMR** (125 MHz, DMSO-d_6): δ 47.6, 55.9, 61.2, 69.6, 115.0, 128.1, 128.2, 128.9, 130.5, 132.6, 137.8, 157.0. **HRMS** (ESI-TOF, m/z) calcd for $C_{32}H_{35}N_2O_2$ $(M + H)^+$ = 479.2693, found 479.2680. **HPLC** (retention time, purity): 30.69 min, 96%.

5.2.1.8. (2S,5S)-2,5-dibenzylpiperazine (5a)[71–76]. Yellow powder, 75% yield. **mp** = 162 °C. **^{1}H NMR** (500 MHz, DMSO-d_6): δ 3.02–3.15 (m, 6H), 3.36–3.47 (m, 4H), 7.29–7.33 (m, 6H), 7.36–7.39 (m, 4H). **^{13}C NMR** (126 MHz, $CDCl_3$) δ 36.4, 44.0, 53.7, 127.0, 128.8, 129.3, 136.5. **HRMS** (ESI-TOF, m/z): calcd for $C_{18}H_{23}N_2$ $(M + H)^+$ = 267.1856, found 267.2196. **HPLC** (retention time, purity): 13.47 min, 99%.

5.2.1.9. (2R,5R)-2,5-dibenzylpiperazine (5b). Yellow powder, 71% yield. **mp** = 162 °C. **^{1}H NMR** (500 MHz, DMSO-d_6): δ 3.02–3.15 (m, 6H), 3.36–3.47 (m, 4H), 7.28–7.33 (m, 6H), 7.36–7.39 (m, 4H). **^{13}C NMR** (126 MHz, DMSO-d_6) δ 34.5, 41.5, 52.4, 127.6, 129.2, 129.8, 136.1. **HRMS** (ESI-TOF, m/z): calcd for $C_{18}H_{23}N_2$ $(M + H)^+$ = 267.1856, found 267.2460. **HPLC** (retention time, purity): 13.57 min, 99%.

5.2.1.10. (2S,5R)-2,5-dibenzylpiperazine (5c). Pale yellow powder, 80% yield. **mp** = 163 °C. **^{1}H NMR** (400 MHz, DMSO-d_6): δ = 1.72 (s, 1H), 2.49 (ddd, J = 24.4, 12.3, 9.3 Hz, 4H), 2.68 (dd, J = 13.4, 5.1 Hz, 2H), 2.85–2.92 (m, 2H), 2.95 (dd, J = 11.3, 2.7 Hz, 2H), 7.15–7.23 (m, 6H), 7.25–7.30 (m, 4H). **^{13}C NMR** (101 MHz, $CDCl_3$): δ = 40.8, 52.6, 57.0, 126.4, 128.5, 129.2, 138.4. **HRMS** (ESI-TOF, m/z): calcd for $C_{18}H_{23}N_2O_2$ $(M + H)^+$ = 267.1856 , found 267.1865. **HPLC** (retention time, purity): 12.74 min, 96%.

5.2.2. General procedure for the synthesis of N,N'-dimethyl-1,4-piperazines

A 1,4-piperazines was dissolved in formic acid (50 equiv.) in a regular round bottom flask and stirred for a few minutes. Formaldehyde (33 equiv, 37% v/v in water) was added and the mixture was stirred at 70 % C for 30 min. EtOAc was used to dilute the reaction mixture and a saturated $NaHCO_3$ solution was added dropwise until no further gas formation was observed. The reaction mixture was extracted three times with EtOAc. The organic layers were combined, dried with Na_2SO_4, filtered, and concentrated *in vacuo*, giving *N,N'*-dimethyl-1,4-piperazines with 74% to 80% yields . Crude products were purified by flash chromatography using (90:5:5) CH_2Cl_2/MeOH/AcOH).

5.2.2.1. (2S,5S)-2-benzyl-5-(ρ-(benzyloxy)benzyl)-1,4-dimethylpiperazine (1a')[31]. White powder, 74% yield. **mp** = 111 °C. **^{1}H NMR** (500 MHz, $CDCl_3$): δ = 2.23–2.28 (m, 2H), 2.37 (s, 3H), 2.38 (s, 3H), 2.47–2.56 (m, 3H), 2.58–2.63 (m, 2H), 2.71 (dd, J = 13.2, 9.6 Hz, 2H), 2.78 (dd, J = 13.0, 9.9 Hz, 2H), 2.95 (dd, J = 13.2, 3.5 Hz, 2H), 2.99 (dd, J = 13.0, 3.7 Hz, 2H), 5.07 (s, 2H), 6.92–6.95 (m, 2H), 7.12–7.16 (d,

2H), 7.22–7.24 (m, 3H), 7.29–7.36 (m, 3H), 7.39–7.42 (m, 2H), 7.45–7.47 (m, 2H); **^{13}C NMR** (125 MHz, $CDCl_3$): δ = 32.6, 42.8, 42.9, 55.3, 55.7, 62.8, 63.0, 70.0, 114.7, 125.8, 127.5, 127.9, 128.3, 128.6, 129.4, 130.3, 132.4, 137.2, 140.3, 157.1; **HRMS** (ESI-TOF, *m/z*) calcd for $C_{27}H_{33}N_2O$ $(M + H)^+$ = 401.2587, found 401.2593. **HPLC** (retention time, purity): 29.26 min, 95%.

5.2.2.2. (2S,5S)-2,5-bis(ρ-(benzyloxy)benzyl)-1,4-dimethylpiperazine (3a')[31]. White powder, 75% yield. **mp** = 172 °C. **^{1}H NMR** (500 MHz, $CDCl_3$): δ = 2.24 (dd, *J* = 11.4, 3.0 Hz, 2H), 2.36 (s, 6H), 2.49 (dd, *J* = 11.4, 6.2 Hz, 2H), 2.52–2.57 (m, 2H), 2.70 (dd, *J* = 13.2, 9.7 Hz, 2H), 2.91 (dd, *J* = 13.2, 3.5 Hz, 2H), 5.06 (s, 4H), 6.92 (d, *J* = 8.6 Hz, 4H), 7.13 (d, *J* = 8.6 Hz, 4H), 7.32–7.37 (m, 2H), 7.39–7.41 (m, 4H), 7.44–7.46 (m, 4H); **^{13}C NMR** (125 MHz, $CDCl_3$): δ = 32.0, 42.8, 55.5, 63.9, 114.7, 127.5, 127.9, 128.6, 130.3, 132.4, 137.2, 157.1. **HRMS** (ESI-TOF, *m/z*) calcd for $C_{34}H_{39}N_2O_2$ $(M + H)^+$ = 507.3006, found 507.3011. **HPLC** (retention time, purity): 35.32 min, 96%.

5.2.2.3. (2S,5S)-2,5-dibenzyl-1,4-dimethylpiperazine (5a')[72]. Yellow powder, 80% yield. **mp** = 120 °C. **^{1}H NMR** (500 MHz, $CDCl_3$): δ 2.24 (dd, *J* = 11.6, 3.2 Hz, 2H), 2.37 (s, 6H), 2.50 (dd, *J* = 11.6, 6.2 Hz, 2H), 2.57–2.61 (m, 2H), 2.76 (dd, *J* = 13.0, 9.9 Hz, 2H), 2.99 (dd, *J* = 13.0, 3.7 Hz, 2H), 7.19–7.22 (m, 6H), 7.27–7.31 (m, 4H). **^{13}C NMR** (100 MHz, DMSO-d_6): δ 33.1, 43.0, 55.8, 63.1, 128.1, 128.6, 129.6, 129.7, 140.5. **HRMS** (ESI-TOF, *m/z*) calcd for $C_{20}H_{27}N_2$ $(M + H)^+$ = 295.2169, found 295.2173. **HPLC** (retention time, purity): 19.95 min, 96%.

5.2.2.4. (2R,5R)-2,5-dibenzyl-1,4-dimethylpiperazine (5b'). Pale yellow powder, 78% yield. **mp** = 120 °C. **^{1}H NMR** (400 MHz, $CDCl_3$): δ 2.29 (dd, *J* = 11.8, 3.3 Hz, 2H), 2.38 (s, 6H), 2.52 (dd, *J* = 11.7, 6.2 Hz, 2H), 2.61–2.67 (m, 2H), 2.78 (dd, *J* = 13.0, 9.9 Hz, 2H), 2.99 (dd, *J* = 13.0, 3.7 Hz, 2H), 7.19–7.22 (m, 6H), 7.26–7.31 (m, 4H). **^{13}C NMR** (100 MHz, $CDCl_3$): δ 33.1, 42.8, 55.2, 62.7, 126.0, 128.4, 129.4, 129.7, 139.8. **HRMS** (ESI-TOF, *m/z*) calcd for $C_{20}H_{27}N_2$ $(M + H)^+$ = 295.2169, found 295.2177. **HPLC** (retention time, purity): 19.94 min, 95%.

5.2.2.5. (2R,5S)-2,5-dibenzyl-1,4-dimethylpiperazine (5c'). White powder, 80% yield. **mp** = 123 °C. **^{1}H NMR** (400 MHz, $CDCl_3$): δ 2.26 (dd, *J* = 11.8, 3.0 Hz, 2H), 2.41 (s, 3H), 2.43 (s, 3H), 2.42–2.51 (m, 2H), 2.54–2.59 (m, 2H), 2.83 (dd, *J* = 13.2, 9.8 Hz, 2H), 3.01 (dd, *J* = 13.1, 6.9 Hz, 2H), 7.18–7.24 (m, 6H), 7.23–7.33 (m, 4H). **^{13}C NMR** (100 MHz, $CDCl_3$): δ 32.1, 43.2, 56.8, 63.3, 128.1, 128.5, 129.6, 129.7, 140.5. **HRMS** (ESI-TOF, *m/z*) calcd for $C_{20}H_{27}N_2$ $(M + H)^+$ = 295.2169, found 295.2181. **HPLC** (retention time, purity): 16.00 min, 99%.

5.2.3. General procedure for benzyl hydrogenolysis

The 1,4-piperazines and *N,N'*-dimethyl-1,4-piperazines containing benzylether side chains have been subjected to hydrogenolysis using classical debenzylation procedure using palladium/H_2 chemistry. The benzyl containing piperazine was dissolved in AcOH and placed in a high-pressure vessel. The vessel was installed on an hydrogenator and, after four purges, the H_2 pressure was set at 50 psi at room temperature. After 3 h, the reaction was stopped. The mixture was filtered on Celite® pad. The filtrate was concentrated *in vacuo*. The crude product, if necessary, was purified column chromatography using CH_2Cl_2/MeOH mixture as eluent. The 1,4-piperazines **2a-2b** and **4a-4b** were directly hydrogenated after the reduction of the CDP without purification therefore the yield is reported for those two steps. The *N,N'*-dimethyl-1,4-piperazines **2a'** and **4a'** were directly hydrogenated after the double *N*-methylation of **1a** and **3a** respectively without purification therefore the yield is reported for those two steps.

5.2.3.1. 4-(((2S,5S)-5-benzylpiperazin-2-yl)methyl)phenol (2a). White powder, 64% yield (2 steps). **mp** = 45 °C. **^{1}H NMR** (500 MHz, $CDCl_3$): δ 2.76 (dd, *J* = 13.6, 6.7 Hz, 1H), 2.82–2.91 (m, 5H), 2.94–2.98 (m, 2H), 3.05–3.09 (m, 1H), 3.11–3.16 (m, 1H), 6.67 (d, *J* = 8.4 Hz, 2H), 6. 99 (d, *J* = 8.4 Hz, 2H), 7.21–7.25 (m, 3H), 7.30–7.33 (m, 2H). **^{13}C NMR** (125 MHz, $CDCl_3$): δ 37.8, 46.5, 46.9, 50.8, 54.8, 55.4, 115.8, 126.6, 128.7, 129.2, 129.3, 130.2, 138.3, 155.2. **HRMS** (ESI-TOF, *m/z*) calcd for $C_{18}H_{23}N_2O$ $(M + H)^+$ = 283.1805, found 283.1815. **HPLC** (retention time, purity): 12.40 min, 95%.

5.2.3.2. 4-(((2R,5R)-5-benzylpiperazin-2-yl)methyl)phenol (2b). White powder, 60% yield (2 steps). **mp** = 45 °C. **^{1}H NMR** (500 MHz, $CDCl_3$): δ **^{1}H NMR** (500 MHz, $CDCl_3$): δ 2.76 (dd, *J* = 13.6, 6.7 Hz, 1H), 2.82–2.91 (m, 5H), 2.94–2.98 (m, 2H), 3.05–3.09 (m, 1H), 3.11–3.16 (m, 1H), 6.67 (d, *J* = 8.4 Hz, 2H), 6. 99 (d, *J* = 8.4 Hz, 2H), 7.21–7.25 (m, 3H), 7.30–7.33 (m, 2H). **^{13}C NMR** (125 MHz, $CDCl_3$): δ 37.8, 46.5, 46.9, 50.8, 54.8, 55.4, 115.8, 126.6, 128.7, 129.2, 129.3, 130.2, 138.3, 155.2. **HRMS** (ESI-TOF, *m/z*) calcd for $C_{18}H_{23}N_2O$ $(M + H)^+$ = 283.1805, found 283.1810. **HPLC** (retention time, purity): 12.40 min, 95%.

5.2.3.3. 4,4'-(((2S,5S)-piperazine-2,5-diyl)bis(methylene))diphenol (4a)[74,77]. Beige powder, 60% yield (2 steps). **mp** = 90 °C. **^{1}H NMR** (500 MHz, DMSO-d_6): δ 1.72 (s, 2H), 2.55 (dd, *J* = 17.1, 3.6 Hz, 2H), 2.56–2.62 (m, 4H), 3.35–3.38 (m, 4H), 6.64 (d, *J* = 8.4 Hz, 4H), 6.95 (d, *J* = 8.4 Hz, 4H). **^{13}C NMR** (126 MHz, DMSO-d_6): δ 47.7, 56.1, 61.2, 115.5, 130.1, 130.3, 156.2. **HRMS** (ESI-TOF, *m/z*) calcd for $C_{18}H_{23}N_2O_2$ $(M + H)^+$ = 299.1754, found 299.1764. **HPLC** (retention time, purity): 9.44 min, 95%.

5.2.3.4. 4,4'-(((2R,5R)-piperazine-2,5-diyl)bis(methylene))diphenol (4b). White powder, 58% yield (2 steps). **mp** = 90 °C. **^{1}H NMR** (500 MHz, DMSO-d_6): δ 1.72 (s, 2H), 2.55 (dd, *J* = 17.1, 3.6 Hz, 2H), 2.56–2.62 (m, 4H), 3.35–3.38 (m, 4H), 6.64 (d, *J* = 8.4 Hz, 4H), 6.95 (d, *J* = 8.4 Hz, 4H). **^{13}C NMR** (126 MHz, DMSO-d_6): δ 47.7, 56.1, 61.2, 115.5, 130.1, 130.3, 156.2. **HRMS** (ESI-TOF, *m/z*) calcd for $C_{18}H_{23}N_2O_2$ $(M + H)^+$ = 299.1754, found 299.1762. **HPLC** (retention time, purity): 9.45 min, 96%.

5.2.3.5. 4-(((2S,5S)-5-benzyl-1,4-dimethylpiperazin-2-yl)methyl)phenol (2a'). Brown oil, 58% yield (2 steps). **mp** = 148 °C. **^{1}H NMR** (500 MHz, $CDCl_3$): δ 2.40 (dd, *J* = 11.2, 5.8 Hz, 1H), 2.44 (s, 3H), 2.47 (s, 3H), 2.52–2.54 (m, 2H), 2.61 (dd, *J* = 12.9, 6.0 Hz, 2H), 2.86–2.90 (m, 2H), 2.96–3.03 (m, 3H), 6.73 (d, *J* = 8.5 Hz, 2H), 6.99 (d, *J* = 8.5 Hz, 2H), 7.20–7.25 (m, 3H), 7.30–7.33 (m, 2H). **^{13}C NMR** (125 MHz, $CDCl_3$): δ 18.4, 22.2, 41.7, 42.0, 53.4, 58.5, 61.0, 61.6, 115.7, 126.5, 128.5, 128.6, 129.3, 130.2, 155.7, 176.6. **HRMS** (ESI-TOF, *m/z*) calcd for $C_{20}H_{27}N_2O$ $(M + H)^+$ = 311.2118, found 311.2128. **HPLC** (retention time, purity): 16.60 min, 95%.

5.2.3.6. 4,4'-(((2S,5S)-1,4-dimethylpiperazine-2,5-diyl)bis(methylene)) diphenol (4a'). White powder, 55% yield (2 steps). **mp** = 155 °C. **^{1}H NMR** (400 MHz, DMSO-d_6): δ 2.17 (s, 6H), 2.29 (d, *J* = 8.3 Hz, 4H), 2.44–2.50 (m, 4H), 2.70–2.73 (m, 2H), 6.62 (d, *J* = 8.1 Hz, 4H), 6.91 (d, *J* = 8.1 Hz, 4H), 9.10 (s, 2H). **HRMS** (ESI-TOF, *m/z*) calcd for $C_{20}H_{27}N_2O_2$ $(M + H)^+$ = 327.2027, found 327.2040. **HPLC** (retention time, purity): 12.60 min, 96%.

5.3. Antifungal and antibiofilm assays

Inhibition of biofilm formation and the minimal inhibitory concentration (MIC) were assessed by absorbance spectrometry using the crystal violet staining method in a culture-treated flat-bottom 96-well microplate as previously described.[78] *Candida albicans* ATCC 28,366 and clinical isolate LAM-1 were cultivated overnight at 37 °C in aerobic conditions using Sabouraud media pH 7.0. Optical density at 660 nm (OD_{660}) of the overnight culture was adjusted to 0.2. Then, equal volumes (100 µL) of the microbial suspension and two-fold serial dilutions of the piperazine solutions in culture medium were incubated at 37 °C

for 24 to 48 h in a 96-well plate to allow biofilm formation. After recording the OD_{660} to monitor microbial growth, the culture medium was removed from the wells which were then rinsed with water before staining the biofilm by adding 100 μL of an aqueous solution of crystal violet (0.001%) for 15 min. The wells were rinsed twice with water for dye removal and allowed to dry. The dye was released from biofilm by adding 75% ethanol (100 μL per well) and the biofilm was quantified by measuring the absorbance at 550 nm (A_{550}). Control wells containing no piperazine were included as a reference of maximal planktonic and biofilm growth (100%). Blanks containing no microorganisms were included for each concentration of piperazine as well as controls containing only culture medium. Relative biofilm growth was calculated for each concentration by reporting its A_{550} as a percentage of the A_{550} of wells containing only microorganisms in culture broth (100%) after subtraction of their respective blanks.

A compound possesses antibiofilm properties when a significant reduction in biofilm formation is observed at concentrations not affecting microbial growth. The MIC is the lowest concentration where no microbial growth is visually observed after 24 h. The minimal fungicidal concentration (MFC) is the lowest concentration (≥MIC) that prevents colony growth after inoculation (5 μL per well) on nutritive agar and further incubation (24 h, 37 °C). In the case where the MIC and MFC vary between replicates, the highest value prevails. The results are a mean of at least two independent experiments performed in triplicates. The significance of the results was determined according to *p* values calculated with the *t* Test.

The disruption of pre-established biofilms was assessed by growing *C. albicans* biofilm in Sabouraud pH 7.0 for 36 to 48 h in a culture-treated flat-bottom 96-well microplate in the absence of piperazines. The culture medium and free-floating microorganisms were removed, and the biofilm was rinsed once with 50 mM phosphate-buffered saline (PBS, pH 7.0). Two-fold serial dilutions of piperazines in PBS were added to the preformed mature biofilms. Microplates were further incubated for 12 h, then wells were washed, and residual biofilm stained with crystal violet as described above. Biofilms treated with PBS were used as controls.

5.4. Inhibition of C. Albicans morphogenesis

Fresh cultures of *Candida albicans* were grown overnight in YPD (1% yeast extract, 2% peptone, 2% dextrose) at 30 °C to favor the yeast morphology. Morphogenesis was induced by incubation at 37 °C following yeast suspension in hyphae-inducing media, including: carbon-limiting Spider media (1% nutrient broth, 1% mannitol, 0.2% K_2HPO_4, pH 7.2); minimal amino-acid Lee's media (0.05% L-Ala, 0.13% L-Leu, 0.1% L-Lys, 0.01% L-Met, 0.05% L-Phe, 0.05% L-Pro, 0.05% L-Thr, 0.007% L-ornithine, 1 mg/mL Biotin, 0.5% NaCl, 0.25% K_2HPO_4, 0.5% ammonium sulfate, 1% dextrose); FBS-enriched YPD (1% yeast extract, 2% peptone, 2% dextrose, 10% fetal bovine serum); GlcNAc media (0.5% *N*-acetylglucosamine, 0.5% peptone, 0.3% KH_2PO_4); low-nitrogen SLAD media (YNB without amino acids and ammonium sulfate, 2% raffinose, 7 mg/mL ammonium sulfate);

Two-fold dilutions of piperazines were made in chosen culture medium in a final volume of 5 mL per sample. Each tube was inoculated with 50 μL of overnight cultures of *C. albicans* yeast (YPD, 30 °C) and then incubated at 37 °C for 4 h to induce morphogenesis. The percentage of cells in the hypha and yeast morphotypes was determined by microscopy, counting at least 100 cells for each replicate. Hypha cells were counted as one cell unless a septum was clearly visible. Intermediate shapes such as linear cells and pseudohyphae were counted as hypha cells on the rational basis that their morphology had changed. Budding yeast cells were counted as one cell if the daughter cell was significantly smaller than the mother. A control sample without piperazine was included to indicate maximal conversion. The results are presented as mean ± standard deviation of at least two independent experiments produced in triplicate. After incubation, the OD_{660} was measured to monitor fungal growth, and the viability of *C. albicans* was confirmed by plate count.

5.5. Reduction of C. Albicans adherence

The adherence of *C. albicans* on epithelial cells was evaluated as described by Ben Marquis et al. (2012)[79] using fluorescein isothiocyanate (FITC)-labeled cultures with slight modifications. The GMSM-K human epithelial cells[80] were cultured in Dulbecco's modified Eagle's medium (DMEM) supplemented with 10% heat-inactivated FBS and 100 μg/mL penicillin G/streptomycin and incubated at 37 °C in an atmosphere of 5% CO_2. The cells were seeded in 96-well clear bottom black microplates (100 μL at 1.5×10^6 cells/ml) and incubated overnight to reach confluence.

The *C. albicans* cells were labeled by using an overnight culture (10 mL) of *C. albicans* that was centrifuged at 7000 × g for 10 min and suspended in 12 mL of fresh 0.5 M $NaHCO_3$ (pH 8) containing 0.03 mg/mL of FITC. The suspensions were incubated in the dark at 37 °C for 30 min with constant shaking. Then, the FITC-labeled yeasts were washed three times by centrifugation (7000 × g for 5 min) and suspended in DMEM.

The confluent monolayers of the immortalized human epithelial cell line GMSM-K seeded in 96-well clear-bottom black microplates were pre-incubated with two-fold serial dilutions of piperazines in DMEM for 30 min (37 °C, 5% CO_2). A suspension of FITC-labeled *C. albicans* in DMEM was added to the wells at a multiplicity of infection (MOI) of 10^3 before further incubation for 4 h in the same conditions. The wells were washed twice with PBS to remove unbound microorganisms. Relative fluorescence units (RFU; excitation wavelength 495 nm; emission wavelength 525 nm) corresponding to the level of *Candida* adherence were determined using a Synergy 2 microplate reader. Control wells without piperazines were used to determine 100% adherence values, while wells without microorganisms were used as controls to measure basal autofluorescence. The results were reported as a percentage compared to the control wells containing no piperazine (100% adherence). They are shown as the mean ± standard deviation of the relative fluorescence obtained from two independent experiments produced in triplicate. Pictures were taken with a FSX100 Olympus camera.

In a separate experiment performed in black-bottomed 96-well microplate, the fluorescence of 100 μL solutions of FITC (0.5 μg/mL in PBS) in the absence and presence of piperazines were compared as a control experiment to detect possible interference or fluorescence quenching by the piperazines. Such interference was not observed. FITC concentration was adjusted to 0.5 μg/mL to obtain a fluorescence signal in the same range as in the adherence assay.

5.6. In vitro biocompatibility assay with oral epithelial cells

The human oral epithelial cell line B11, that has been previously characterized[81], was kindly provided by S. Groeger (Justus Liebig University Giessen, Germany). Cells were cultured in keratinocyte serum-free medium (K-SFM; Life Technologies Inc.) supplemented with growth factors (50 μg/mL of bovine pituitary extract and 5 ng/mL of human epidermal growth factor) and 100 μg/mL of penicillin G-streptomycin. The cultures were incubated at 37 °C in a 5% CO_2. To evaluate the effect of compound **1a** on cell viability, cells were seeded (1×10^5 cells in 100 μL) into wells of a 96-well tissue culture plate and incubated at 37 °C in a 5% CO_2 atmosphere until they reached confluence. Cells were treated with two-fold serial dilutions of the compound (from 96 to 1.5 μg/mL) for 2 and 24 h. Thereafter, an MTT (3-[4, 5-diethylthiazol-2-yl]-2,5-diphenyltetrazolium bromide) assay was performed according to the manufacturer's protocol (Roche Diagnostics, Mannheim, Germany) to assess cell viability. The assays were performed in triplicate and the means ± standard deviations were calculated.

Author contributions

C.B. synthesized and characterized the piperazines. P.A.P.C contributed to the synthesis of the piperazines. G.S. performed and analyzed the biological experiments. G.S. and C.B. co-wrote the first draft of the manuscript. P.A.P.C, D.G and N.V revised and edited the manuscript. D.G and N.V. designed and supervised the project and contributed equally to the work. All authors approved the final version of the manuscript.

Declaration of Competing Interest

The authors declare that they have no known competing financial interests or personal relationships that could have appeared to influence the work reported in this paper.

Acknowledgements

This work was supported by Natural Sciences and Engineering Research Council of Canada (NSERC) [grant number RGPIN/04834-2017]; the Fonds de recherche du Québec-Nature et Technologies (FRQNT); the Quebec Network for Research on Protein Function, Engineering, and Applications (PROTEO); and Université Laval. The authors would like to thank Marie-Pier Veilleux and Katy Vaillancourt for her technical support, as well as Geneviève Lebel and Jabrane Azelmat for their useful advice.

Appendix A. Supplementary material

Supplementary data to this article can be found online at https://doi.org/10.1016/j.bmc.2020.115810.

References

1 Nobile CJ, Johnson AD. Candida albicans Biofilms and Human Disease. *Annu Rev Microbiol*. 2015;69:71–92. https://doi.org/10.1146/annurev-micro-091014-104330.
2 Swidergall M, Filler SG. Oropharyngeal Candidiasis: Fungal Invasion and Epithelial Cell Responses. *PLoS Pathog*. 2017;13, e1006056. https://doi.org/10.1371/journal.ppat.1006056.
3 Pfaller MA, Diekema DJ. Epidemiology of Invasive Candidiasis: a Persistent Public Health Problem. *Clin Microbiol Rev*. 2007;20:133–163. https://doi.org/10.1128/CMR.00029-06.
4 Gendreau L, Loewy ZG. Epidemiology and etiology of denture stomatitis. *Int J Prostodont*. 2011;20:251–260. https://doi.org/10.1111/j.1532-849X.2011.00698.x.
5 Moran AC, Grussemeyer RC, Spalding KJ, Benjamin DD, Reed DS. Candida Albicans and Non-Albicans Bloodstream infections in Adult and Pediatric Patients: Comparison of Mortality and Costs. *Pediatr Infect Dis J*. 2009;28:433–435. https://doi.org/10.1097/INF.0b013e3181920ffd.
6 Srivastava V, Singla RK, Dubey AK. Emerging Virulence, Drug Resistance and Future Anti-fungal Drugs for Candida Pathogens. *Curr Top Med Chem*. 2018;18:759–778.
7 Percival S, Suleman L, Vuotto C, Donelli G. Healthcare-associated infections, medical devices and biofilms: risk, tolerance and control. *J Med Microbiol*. 2015;64:323–334. https://doi.org/10.1099/jmm.0.000032.
8 Ramage G, Martínez JP, López-Ribot JL. Candida biofilms on implanted biomaterials: a clinically significant problem. *FEMS Yeast Res*. 2006;6:979–986. https://doi.org/10.1111/j.1567-1364.2006.00117.x.
9 Kojic E, Darouiche R. Candida Infections of Medical Devices. *Clin Microbiol Rev*. 2004;17:255–267. https://doi.org/10.1128/CMR.17.2.255-267.2004.
10 Wisplinghoff H, Bischoff T, Tallent SM, Seifert H, Wenzel RP, Edmond MB. Nosocomial bloodstream infections in US hospitals: analysis of 24,179 cases from a prospective nationwide surveillance study. (Major Article). *Clin Infect Dis*. 2004;39:309–317. https://doi.org/10.1086/421946.
11 Sudbery P, Gow N, Berman J. The distinct morphogenic states of Candida albicans. *Trends Microbiol*. 2004;12:317–324. https://doi.org/10.1016/j.tim.2004.05.008.
12 Shareck J, Belhumeur P. Modulation of Morphogenesis in Candida albicans by Various Small Molecules. *Eukaryot Cell*. 2011;10:1004–1012. https://doi.org/10.1128/EC.05030-11.
13 Gulati M, Nobile CJ. Candida albicans biofilms: development, regulation, and molecular mechanisms. *Microbes Infect*. 2016;18:310–321. https://doi.org/10.1016/j.micinf.2016.01.002.
14 Uppuluri P, Chaturvedi AK, Srinivasan A, et al. Dispersion as an Important Step in the Candida albicans Biofilm Developmental Cycle. *PLoS Pathog*. 2010;6, e1000828. https://doi.org/10.1371/journal.ppat.1000828.
15 Andes D, Safdar N, Baddley JW, et al. Impact of Treatment Strategy on Outcomes in Patients with Candidemia and Other Forms of Invasive Candidiasis: A Patient-Level Quantitative Review of Randomized Trials. *Clin Infect Dis*. 2012;54:1110–1122. https://doi.org/10.1093/cid/cis021.
16 Cornely OA, Bassetti M, Calandra T, et al. ESCMID* guideline for the diagnosis and management of Candida diseases 2012: non-neutropenic adult patients. *Clin Microbiol Infect*. 2012;18:19–37. https://doi.org/10.1111/1469-0691.12039.
17 Tumbarello M, Fiori B, Trecarichi EM, et al. Risk Factors and Outcomes of Candidemia Caused by Biofilm-Forming Isolates in a Tertiary Care Hospital (Biofilm Candida Infection and Outcomes). *PLoS ONE*. 2012;7, e33705. https://doi.org/10.1371/journal.pone.0033705.
18 Pappas PG, Kauffman C, Andes D, et al. Clinical Practice Guidelines for the Management of Candidiasis: 2009 Update by the Infectious Diseases Society of America. *Clin Infect Dis*. 2009;48:503–535. https://doi.org/10.1086/596757.
19 Seddiki SML, Boucherit-Otmani Z, Boucherit K, Kunkel D. Fungal infectivities of implanted catheters due to Candida sp. Biofilms formation and resistance. *J Med Mycol*. 2015;25:130–135. https://doi.org/10.1016/j.mycmed.2015.03.003.
20 Vediyappan G,Rossignol T,apos,Enfert C. Interaction of Candida albicans Biofilms with Antifungals: Transcriptional Response and Binding of Antifungals to Beta-Glucans. Antimicrob. Agents Chemother. 2010;54:2096-2111. https://doi.org/10.1128/AAC.01638-09.
21 Nett J, Lincoln L, Marchillo K, et al. Putative Role of {beta}-1,3 Glucans in Candida albicans Biofilm Resistance. *Antimicrob Agents Chemother*. 2007;51:510. https://doi.org/10.1128/AAC.01056-06.
22 Nett JE, Crawford K, Marchillo K, Andes DR. Role of Fks1p and Matrix Glucan in Candida albicans Biofilm Resistance to an Echinocandin, Pyrimidine, and Polyene. *Antimicrob Agents Chemother*. 2010;54:3505–3508. https://doi.org/10.1128/AAC.00227-10.
23 Tsui C,Kong EF,Jabra-Rizk MA. Pathogenesis of Candida albicans biofilm. Pathog. Dis. 2016;74:ftw018.
24 Bonhomme J,D'enfert C. Candida albicans biofilms: building a heterogeneous, drug-tolerant environment. Curr. Opin. Microbiol. 2013;16:398-403. https://doi.org/10.1016/j.mib.2013.03.007.
25 Cavalheiro M, Teixeira MC. Biofilms: Threats, Challenges, and Promising Strategies. *Front Med*. 2018;5:28. https://doi.org/10.3389/fmed.2018.00028.
26 Taylor RD, MacCoss M, Lawson AD. Rings in drugs. *J Med Chem*. 2014;57:5845–5859. https://doi.org/10.1021/jm4017625.
27 Shaquiquzzaman M, Verma G, Marella A, et al. Piperazine scaffold: A remarkable tool in generation of diverse pharmacological agents. *Eur J Med Chem*. 2015;102:487–529. https://doi.org/https://doi.org/10.1016/j.ejmech.2015.07.026.
28 de Carvalho MP, Abraham WR. Antimicrobial and biofilm inhibiting diketopiperazines. *Curr Med Chem*. 2012;19:3564–3577.
29 Martins MB, Carvalho I. Diketopiperazines: biological activity and synthesis. *Tetrahedron*. 2007;63:9923–9932. https://doi.org/https://doi.org/10.1016/j.tet.2007.04.105.
30 Simon G, Bérubé C, Voyer N, Grenier D. Anti-biofilm and anti-adherence properties of novel cyclic dipeptides against oral pathogens. *Bioorg Med Chem*. 2019;27:2323–2331. https://doi.org/https://doi.org/10.1016/j.bmc.2018.11.042.
31 Bérubé C, Cardinal S, Boudreault PL, et al. Novel chiral N, N'-dimethyl-1,4-piperazines with metal binding abilities. *Tetrahedron*. 2015;71:8077–8084.
32 Bérubé C, Barbeau X, Cardinal S, et al. Interfacial supramolecular biomimetic epoxidation catalyzed by cyclic dipeptides. *Supramol Chem*. 2017;29:330–349.
33 Bérubé C, Carpentier C, Voyer N. Total synthesis of chrysamide B. *Tetrahedron Lett*. 2017;58:2334–2336. https://doi.org/http://doi.org/10.1016/j.tetlet.2017.04.079.
34 Bérubé C, Voyer N. Crown-ether-modified cyclic dipeptides as supramolecular chiral catalysts. *Supramol Chem*. 2018;30:184–195. https://doi.org/10.1080/10610278.2017.1392521.
35 DeGrado WF, Kaiser ET. Polymer-bound oxime esters as supports for solid-phase peptide synthesis. The preparation of protected peptide fragments. *J Org Chem*. 1980;45:1295–1300. https://doi.org/10.1021/jo01295a026.
36 DeGrado WF, Kaiser ET. Solid-phase synthesis of protected peptides on a polymer-bound oxime: preparation of segments comprising the sequence of a cytotoxic 26-peptide analog. *J Org Chem*. 1982;47:3258–3261. https://doi.org/10.1021/jo00138a011.
37 Kopac DS, Hall DG. General solid-phase approach to the synthesis of chiral triazacycloalkane ligands with stereogenic backbone substituents. *J Comb Chem*. 2002;4:251.
38 Nystrom RF. Reduction of organic compounds by lithium aluminum hydride; halides, quinones, miscellaneous nitrogen compounds. *J Am Chem Soc*. 1948;70:3738–3740.
39 Eschweiler W. *Ber Dtsch Chem Ges*. 1905;38:880.
40 Ramage G, VandeWalle K, López-Ribot JL, Wickes BL. The filamentation pathway controlled by the Efg1 regulator protein is required for normal biofilm formation and development in Candida albicans. *FEMS Microbiol Lett*. 2002;214:95–100. https://doi.org/10.1111/j.1574-6968.2002.tb11330.x.
41 Desai JV, Mitchell AP. Candida albicans Biofilm Development and Its Genetic Control. *Microbiol. Spectr*. 2015;3. https://doi.org/10.1128/microbiolspec.MB-0005-2014, 10.1128/microbiolspec.MB-0005-2014.
42 Han T-L, Cannon RD, Villas-Bôas SG. The metabolic basis of Candida albicans morphogenesis and quorum sensing. *Fungal Genet Biol*. 2011;48:747–763. https://doi.org/10.1016/j.fgb.2011.04.002.
43 Midkiff J,Borochoff-Porte N,White D,Johnson DI. Small Molecule Inhibitors of the Candida albicans Budded-to-Hyphal Transition Act through Multiple Signaling Pathways (C. albicans BHT Inhibitors Block Multiple Pathways). PloS One 2011;6:e25395. https://doi.org/10.1371/journal.pone.0025395.
44 Nadeem SG,Shafiq A,Hakim ST,Anjum Y,Kazm SU. Effect of growth media, pH and temperature on yeast to hyphal transition in Candida albicans. Open J. Med. Microbiol. 2013;3:185-192, 188 pp. https://doi.org/10.4236/ojmm.2013.33028.

45 Lee KL, Buckley HR, Campbell CC. An amino acid liquid synthetic medium for the development of mycellal and yeast forms of Candida albicans. *J. Med. Mycol.* 1975; 13:148–153. https://doi.org/10.1080/00362177585190271.

46 Sandini S, Stringaro A, Arancia S, et al. The MP65 gene is required for cell wall integrity, adherence to epithelial cells and biofilm formation in Candida albicans, 106-106 *BMC Microbiol.* 2011;11. https://doi.org/10.1186/1471-2180-11-106.

47 Fox EP, Bui CK, Nett JE, et al. An expanded regulatory network temporally controls Candida albicans biofilm formation. *Mol Microbiol.* 2015;96:1226–1239. https://doi.org/10.1111/mmi.13002.

48 Matthew BL, Megha G, Alexander DJ, Clarissa JN. Development and regulation of single- and multi-species Candida albicans biofilms. *Nat Rev Microbiol.* 2017;16: 19–31. https://doi.org/10.1038/nrmicro.2017.107.

49 Nobile Clarissa j,Fox Emily p,Nett Jeniel e,Sorrells Trevor r,Mitrovich Quinn m, Hernday Aaron d,Tuch Brian b,Andes David r,Johnson Alexander d. A Recently Evolved Transcriptional Network Controls Biofilm Development in Candida albicans. Cell 2012;148:126-138. https://doi.org/10.1016/j.cell.2011.10.048.

50 Kadosh D. Control of Candida albicans morphology and pathogenicity by post-transcriptional mechanisms. *Cell Mol Life Sci.* 2016;73:4265–4278. https://doi.org/10.1007/s00018-016-2294-y.

51 Morschhäuser J. Nitrogen regulation of morphogenesis and protease secretion in Candida albicans. *Int J Med Microbiol*. 2011;301:390–394. https://doi.org/https://doi.org/10.1016/j.ijmm.2011.04.005.

52 Parsek MR, Greenberg EP. Sociomicrobiology: the connections between quorum sensing and biofilms. *Trends Microbiol*. 2005;13:27–33. https://doi.org/10.1016/j.tim.2004.11.007.

53 Dranginis AM, Rauceo JM, Coronado JE, Lipke PN. A Biochemical Guide to Yeast Adhesins: Glycoproteins for Social and Antisocial Occasions. *Microbiol Mol Biol Rev*. 2007;71:282–294. https://doi.org/10.1128/MMBR.00037-06.

54 Frade JP, Arthington-Skaggs BA. Effect of serum and surface characteristics on Candida albicans biofilm formation. *Mycoses*. 2011;54, e154. https://doi.org/10.1111/j.1439-0507.2010.01862.x.

55 Paula SS, Robert Y, Jonathan DT, et al. Structural basis for the broad specificity to host-cell ligands by the pathogenic fungus Candida albicans. *PNAS*. 2011;108: 15775–15779. https://doi.org/10.1073/pnas.1103496108.

56 Alves CT, Silva S, Pereira L, Williams DW, Azeredo J, Henriques M. Effect of progesterone on Candida albicans vaginal pathogenicity. *Int J Med Microbiol*. 2014; 304:1011–1017. https://doi.org/10.1016/j.ijmm.2014.07.004.

57 Biswas S, Van Dijck P, Datta A. Environmental Sensing and Signal Transduction Pathways Regulating Morphopathogenic Determinants of Candida albicans. *Microbiol Mol Biol Rev*. 2007;71:348–376. https://doi.org/10.1128/MMBR.00009-06.

58 Peter ES. Growth of Candida albicans hyphae. *Nat Rev Microbiol.* 2011;9:737. https://doi.org/10.1038/nrmicro2636.

59 Song Y, Cheon SA, Lee KE, et al. Role of the RAM network in cell polarity and hyphal morphogenesis in Candida albicans. *Mol Biol Cell.* 2008;19:5456–5477. https://doi.org/10.1091/mbc.E08-03-0272.

60 Alvarez FJ, Konopka JB, Lew D. Identification of an N-Acetylglucosamine Transporter That Mediates Hyphal Induction in Candida albicans. *Mol Biol Cell.* 2006; 18:965–975. https://doi.org/10.1091/mbc.e06-10-0931.

61 Biswas K, Morschhäuser J. The Mep2p ammonium permease controls nitrogen starvation-induced filamentous growth in Candida albicans. *Mol Microbiol.* 2005;56: 649–669. https://doi.org/10.1111/j.1365-2958.2005.04576.x.

62 Su C, Yu J, Lu Y. Hyphal development in Candida albicans from different cell states. *Curr Genet.* 2018;64:1239–1243. https://doi.org/10.1007/s00294-018-0845-5.

63 Naseem S, Min K, Spitzer D, Gardin J, Konopka JB. Regulation of Hyphal Growth and N-Acetylglucosamine Catabolism by Two Transcription Factors in. *Genetics*. 2017; 206:299–314. https://doi.org/10.1534/genetics.117.201491.

64 Martin R,Albrecht-Eckardt D,Brunke S,Hube B,Hunniger K,Kurzai O. A Core Filamentation Response Network in Candida albicans Is Restricted to Eight Genes. (Research Article). PloS One 2013;8:e58613. https://doi.org/10.1371/journal.pone.0058613.

65 Marsh PD, Head DA, Devine DA. Ecological Approaches to Oral Biofilms: Control without Killing. *Caries Res*. 2015;49:46–54. https://doi.org/10.1159/000377732.

66 Johnson BK, Abramovitch RB. Small Molecules That Sabotage Bacterial Virulence. *Trend Pharmacol Sci*. 2017;38:339–362. https://doi.org/10.1016/j.tips.2017.01.004.

67 Gauwerky K, Borelli C, Korting HC. Targeting virulence: A new paradigm for antifungals. *Drug Discov Today*. 2009;14:214–222. https://doi.org/10.1016/j.drudis.2008.11.013.

68 Calugi C, Trabocchi A, Guarna A. Novel small molecules for the treatment of infections caused by Candida albicans : a patent review (2002 2010). *Expert Opin Ther Pat.* 2011;21:381–397. https://doi.org/10.1517/13543776.2011.551116.

69 Lebeaux D, Ghigo J, Beloin C. Biofilm-Related Infections: Bridging the Gap between Clinical Management and Fundamental Aspects of Recalcitrance toward Antibiotics. *Microbiol Mol Biol Rev*. 2014;78:510–543. https://doi.org/10.1128/MMBR.00013-14.

70 Cleary JL, Condren AR, Zink KE, Sanchez LM. Calling All Hosts: Bacterial Communication In Situ. *Chem*. 2017;2:334–358. https://doi.org/10.1016/j.chempr.2017.02.001.

71 Li-Hua Q, Zong-Xuan S, Wu-Hong C, Yong Z, Ya-Wen Z. A Convenient Approach to the Enantiopure (15,25,45,55)-and (1R,2S,4R,5S)-2,5-Bis(phenylmethyl)-l,4-diazabicyclo[2.2.2]-octane. *Chin J Chem*. 2003;21:1098–1100. https://doi.org/10.1002/cjoc.20030210824.

72 Selvakumar S, Sivasankaran D, Singh VK. Enantioselective Henry reaction catalyzed by C2-symmetric chiral diamine–copper(II) complex. *Org Biomol Chem*. 2009;7:3156. https://doi.org/10.1039/b904254g.

73 Marichev KO, Takacs JM. Ruthenium-Catalyzed Amination of Secondary Alcohols Using Borrowing Hydrogen Methodology. *ACS Catal*. 2016;6:2205–2210. https://doi.org/10.1021/acscatal.6b00175.

74 Jung ME, Rohloff JC. Organic chemistry of L-tyrosine. 1. General synthesis of chiral piperazines from amino acids. *J Org Chem*. 1985;50:4909–4913. https://doi.org/10.1021/jo00224a051.

75 Soai K, Oshio A, Yoneyama H. Synthesis of (2S,5S)-2,5-bis(phenylmethyl)-1,4-diazabicyclo[2.2.2]octane. *Tetrahedron Asymmetry*. 1992;3:359–360.

76 Soai K, Hayashi H, Shinozaki A, Umebayashi H, Yamada Y. Asymmetric Synthesis Using Chiral Piperazine. I. Asymmetric Synthesis of 2-Substituted Alcohol and Carboxylic Acid by Diastereoselective Alkylation of Chiral Diamides Derived from Piperazines. *Bull Chem Soc Jpn*. 1987;60:3450–3452. https://doi.org/10.1246/bcsj.60.3450.

77 Forseth RR, Amaike S, Schwenk D, et al. Homologous NRPS-like gene clusters mediate redundant small-molecule biosynthesis in Aspergillus flavus. *Angew Chem Int Ed.* 2013;52:1590–1594. https://doi.org/10.1002/anie.201207456.

78 Ben Lagha A, Dudonné S, Desjardins Y, Grenier D. Wild Blueberry (Vaccinium angustifolium Ait.) Polyphenols Target Fusobacterium nucleatum and the Host Inflammatory Response: Potential Innovative Molecules for Treating Periodontal Diseases. *J Agric Food Chem*. 2015;63:6999–7008. https://doi.org/10.1021/acs.jafc.5b01525.

79 Marquis A, Genovese S, Epifano F, Grenier D. The plant coumarins auraptene and lacinartin as potential multifunctional therapeutic agents for treating periodontal disease. *BMC Complement Altern Med*. 2012;12:80. https://doi.org/10.1186/1472-6882-12-80.

80 Gilchrist EP, Moyer MP, Shillitoe EJ, Clare N, Murrah VA. Establishment of a human polyclonal oral epithelial cell line. *Oral Surg Oral Med Oral Pathol Oral Radiol Endod*. 2000;90:340–347. https://doi.org/10.1067/moe.2000.107360.

81 Gröger S, Michel J, Meyle J. Establishment and characterization of immortalized human gingival keratinocyte cell lines. *J Periodontal Res*. 2008;43:604–614. https://doi.org/10.1111/j.1600-0765.2007.01019.x.